World Academy of Science, Engineering and Technology
International Journal of Physical and Mathematical Sciences
Vol:17, No:1, 2023

Simulation of the Asphaltene Deposition Rate in a Wellbore Blockage via Computational Fluid Dynamics

Xiaodong Gao, Pingchuan Dong, Qichao Gao

***Abstract*—**This work attempts to predict the deposition rate of asphaltene particles in blockage tube through CFD simulation. The Euler-Lagrange equation has been applied during the flow of crude oil and asphaltene particles. The net gravitational force, virtual mass, pressure gradient, Saffman lift, and drag forces are incorporated in the simulations process. Validation of CFD simulation results is compared to the benchmark experiments from the previous literature. Furthermore, the effects of blockage location, blockage length, and blockage thickness on deposition rate are also analyzed. The simulation results indicate that the maximum deposition rate of asphaltene occurs in the blocked tube section, and the greater the deposition thickness, the greater the deposition rate. Moreover, the deposition amount and maximum deposition rate along the length of the tube have the same trend. Results of this study are in the ability to better understand the deposition of asphaltene particles in production and help achieve to deal with the asphaltene challenges.

***Keywords*—**Asphaltene deposition rate, blockage length, blockage thickness, blockage diameter, transient condition.

I. Introduction

ASPHALTENE deposition is a more challenging flow assurance issue in the oil-gas production and transportation. Asphaltene can deposit in the reservoir, near the wellbore region, wellbore, production pipeline, and surface facilities since it is influenced by pressure, temperature, composition, and electrokinetic properties [1]-[3]. These adverse phenomena can partially or fully clog the available cross-sectional flow area of wellbores, but also lead to substantial monetary losses and safety problems [4]. It was reported that 2/3 of the tubing cross-sectional area was blocked by asphaltene deposits in the Hassi Messaoud field [5]. Some more efficient and cost-effective manners must therefore be chosen to remove or inhibit the asphaltene deposits in order to reduce the risk of production. Before selecting a scavenger or inhibitor, however, it is necessary to conduct a proper study of asphaltene deposits in the tubing. Based on the reservoir characteristics and well production parameters of the target well, we can study the transportation and deposition of asphaltene particles in tubing and determine the location and amount of deposition.

To date, to better understand the characteristics of asphaltene deposition on interior wall of wellbores, a variety of methods have been proposed to study asphaltene deposition. The first way is to utilize experimental methods, such as capillary deposition flow loop, quartz crystal microbalance, RealView deposition cell, and packed bed column [6]-[12]. Another approach to predict asphaltene deposition is the theoretical, simulation method. The main advantages of this method are lower cost, lower operational difficulty and easier implementation than experimental methods.

Zhu et al. [13] utilized 3D CFD model to predict the distribution of asphaltene deposition in different diametral pipelines. The governing equations of oil-gas-water three-phase flow, realizable k-ε turbulence model and deposition model were combined to measure the deposition rate of asphaltene. They found that multiphase flow in sudden expansion, contraction and bent pipes was more likely to induce asphaltene deposition. Haghshenasfard and Hooman [14] investigated the deposition rate of asphaltene precipitation under forced convection in a vertical tube. Their model was also validated with the experimental data of Jamialahmadi et al. [15]. However, the effect of the particle size, different forces on asphaltene deposition rate were neglected.

Subsequently, based on Eulerian-Lagrangian method, the aggregates with sizes in the range of 50-400 μm were selected to study asphaltene deposition by Seyyedbagheri and Mirzayi [16]. In that work the effect of crude oil velocity, surface roughness, and asphaltene particles number were investigated. The results demonstrated that higher crude oil velocity and particle number favor the deposition rate of asphaltene particles, while roughness enhancement only works for particles with sizes less than 20 μm. At the same time, they [17] also modeled asphaltene deposition process in turbulent production pipeline using Eulerian model. The diffusion, turbophoresis, and thermophoresis mechanisms were incorporated over a wide range of asphaltene particle (1 nm - 100 μm). Another significant work was done by Emani & Ramasamy [18], the gravity, drag, Saffman lift as well as thermophoretic applied on asphaltene particle were considered. Their findings showed that gravitation was the main force for particle deposition on the heat surfaces, and Saffman lift was the dominant force for particles entrainment into the bulk fluid phase. Unfortunately, they did not take into account the interactions between particles. Bagherzadeh et al. [19]

Xiaodong Gao and Pingchuan Dong* are with College of Petroleum Engineering, China University of Petroleum (Beijing), Beijing, China and with State Key Laboratory of Petroleum Resources and Prospecting, China University of Petroleum (Beijing), Beijing, China (*e-mail: dpcfem@163.com).

Qichao Gao is with Sinopec Research Institute of Petroleum Engineering, Beijing 100083, China.

developed a coupled CFD-DEM (Discrete Element Method) model to investigate the agglomeration and fragmentation of asphaltene particles in steady condition. The asphaltene particle-particle collisions, particle-floc collisions, and floc-floc collisions were taken into consideration to determine corresponding collision efficiencies. Moreover, the effect of velocity, concentration of primary asphaltene particles, and the properties of asphaltene flocs were investigated. According to the obtained results, the contribution of particle-particle collisions decreased firstly and then reached a plateau condition. For particle-flocs collisions, the contribution increased initially and then kept decreasing; the contribution of floc-floc collision efficiency continuously increased. Based on the multi-fluid approach, Maddahian et al. [20] investigated the asphaltene deposition and the fouling layer growth in crude oil preheat trains. The numerical results showed that the growth of the fouling layer reduces the cross-sectional area of the pipe and heat transfer coefficient, resulting in an increase in the flow velocity. The key limitation of this research is that they simulated a tube with a 23.8 mm diameter, which is not a realistic tubing size.

Gao et al. [21] carried out a numerical study for asphaltene particle deposition over a wide range of 10-200 μm within a vertical tube. A smooth vertical tube with an inner diameter of 62 mm was developed. The results showed that the Saffman lift force, virtual mass force, and pressure gradient force played a critical role in the asphaltene deposition since the density (1100 kg/m^3) of asphaltenes particle is relatively close to that of crude oil (866 kg/m^3). In addition, the increase in particle size, roughness increased the deposition rate. Mohammad et al. [22] presented an improved Eulerian deposition model that takes the gravity term into account in Guha's advection-diffusion model to predict solid deposition rate. In that work, the molecular, turbulent diffusion, turbophoresis, thermophoresis, and surface roughness were incorporated in inclined and horizontal pipes. They concluded that gravitational setting was the dominated mechanism for asphaltene deposition in laminar flow. Consideration of particle size distribution and aggregation function was beneficial for predicting high-precision asphaltene deposition profiles. These studies mentioned above laid the foundation for asphaltene particles transportation and deposition in production.

Although many related theoretical researches [13], [14], [19], [21] have been conducted for the investigation of asphaltene particle deposition in smooth tubes, the study for investigating the deposition rate and deposition amount of asphaltene particles in blockage wellbores has not been well elucidated. This is particularly significant, since it is reported that asphaltene precipitation are more likely to deposit in shrink tubes [23]. Furthermore, the above studies focused on some stable flow patterns, which fail to consider the time-dependent effects. In this paper, a blockage tube in vertical orientation is established. The Eulerian-Lagrangian model is conducted to describe the motion and deposition of fluid and asphaltene particles at transient condition. In addition, the main factors affecting the deposition rate of asphaltene particle, such as blockage length, thickness, and location, are also studied.

II. Mathematical Model of Blockage

A. Crude Oil Phase Model

The deposition model is based on the following: (1) Heat transfer inside the tubing is not considered; (2) Since the volume fraction of the asphaltene particles is very low ($\leq 10^{-6}$), the particle does not have the considerable influence on the turbulence, so the interactions between asphaltene particles and turbulence were treated as one-way coupling [24]; (3) The asphaltene particles are assumed to deposit onto a wall once they touch the wall. The mass and momentum equations in a transient state condition can be written as:

$$\frac{\partial \rho_f}{\partial t} + \nabla.\left(\rho_f v_f\right) = 0 \tag{1}$$

$$\frac{\partial (\rho_f v_f)}{\partial t} + \nabla\bullet(\rho_f v_f v_f) = -\nabla p_f + \rho_f g + \nabla\bullet(\tau_f) \tag{2}$$

where the subscript f means crude oil; v_f is the mean velocity of fluid phase; p is the pressure of crude oil; g is the acceleration of gravity; τ is the viscous pressure.

B. Asphaltene Particles' Movement

In this paper, asphaltene particles are treated as a discrete phase, so the Lagrangian model is used to track the trajectory of asphaltene precipitation. The drag force, gravity force, buoyancy force, virtual mass force, pressure gradient force, and Saffman lift force are taken into consideration for each asphaltene particle injected into the tube. The velocity change is determined by the force balance on the asphaltene particle, which can be written as:

$$m_p \frac{du_p}{dt} = F_D + m_p g(1 - \frac{\rho_f}{\rho_p}) + F_{vmf} + F_{pgd} + F_{saf} \tag{3}$$

where m_p is the asphaltene particles mass; u_p is the asphaltene particle phase velocity; ρ_p is the density of asphaltene particle; F_D represents the drag force; F_{vmf} is the virtual mass force vector; F_{pdf} is the pressure gradient force vector and F_{saf} is the Saffman lift force vector.

The drag force was calculated as,

$$F_D = m_p \frac{u - v}{\tau_p} \tag{4}$$

τ_p is the asphaltene particle relaxation time calculated by:

$$\tau_p = \frac{\rho_p d_p^{\,2}}{18\mu} \frac{24}{C_d \,\mathrm{Re}_p} \tag{5}$$

μ is the fluid viscosity, d_p is the asphaltene particle diameter; C_d is the drag coefficient; Re_p is the particle Reynolds number. The correlation of non-spherical asphaltene particles is developed by Haider and Levenspiel [25].

$$C_d = \begin{cases} \dfrac{24}{\mathrm{Re}_p}, \mathrm{Re}_p < 1 \\ \dfrac{24}{\mathrm{Re}_p}(1 + b_1 \mathrm{Re}_p^{\,b_2}) + \dfrac{b_3 \mathrm{Re}_p}{b_4 + \mathrm{Re}_p}, 1 < \mathrm{Re}_p < 1000 \\ 0.44, \mathrm{Re}_p > 1000 \end{cases} \quad (6)$$

where,

$$\begin{aligned} b_1 &= \exp(2.3288 - 6.4581\varphi + 2.4486\varphi^2) \\ b_2 &= 0.0964 + 0.5565\varphi \\ b_3 &= \exp(4.905 - 13.8944\varphi + 18.4222\varphi^2 - 10.2599\varphi^3) \\ b_4 &= \exp(1.4681 + 12.2584\varphi - 20.7322\varphi^2 + 15.8855\varphi^3) \end{aligned} \quad (7)$$

The shape factor is defined as

$$\varphi = \frac{s}{S} \quad (8)$$

where s, S are the surface area of a sphere having the same volume as the particle, actual surface area of the particle, respectively.

Gravitational and buoyancy forces are the opposite forces acting on asphaltene particles, which are expressed as:

$$F_G = \frac{\pi}{6} d_p^{\,3} \left(\rho_p - \rho_f \right) g \quad (9)$$

The virtual mass force and pressure gradient force become significant and they are recommended since the density of asphaltene particle is close to the density of crude oil. The virtual mass force and pressure gradient force can be written as:

$$F_{vmf} = 0.5 m_p \frac{\rho_f}{\rho_p} \left(\vec{u}_p \nabla \vec{u} - \frac{d\vec{u}_p}{dt} \right) \quad (10)$$

$$F_{pgf} = m_p \frac{\rho_f}{\rho_p} \vec{u} \nabla \vec{u} \quad (11)$$

The expression of Saffman lift force can be defined as [26]:

$$F_{saf} = \frac{1.615 \mu d_p^{\,2} (du/dr)}{\sqrt{v|du/dr|}} (u - u_p) \quad (12)$$

C. Turbulence Model

Since the k-ω model is more advantageous for wall-restricted boundary layer and bulk flow, and can more accurately predict particle deposition, the transport equations adopted in this work are the Shear Stress Transport (SST) k-ω model [21]. The governing equations of the turbulence model can be written as:

$$\frac{\partial}{\partial t}(\rho k) + \frac{\partial}{\partial x_i}(\rho k u_i) = \frac{\partial}{\partial x_j}\left[(\mu + \frac{\mu_t}{\sigma_k}) \frac{\partial k}{\partial x_j} \right] + G_k - Y_K + G_b \quad (13)$$

$$\frac{\partial}{\partial t}(\rho \omega) + \frac{\partial}{\partial x_i}(\rho \omega u_i) = \frac{\partial}{\partial x_j}\left[(\mu + \frac{\mu_t}{\sigma_\omega}) \frac{\partial \omega}{\partial x_j} \right] + G_\omega - Y_\omega + D_\omega + G_{\omega b} \quad (14)$$

where G_k is the turbulence kinetic energy caused by mean velocity gradients; Y_K is the dissipation of k due to turbulence; G_b is the turbulence generation due to buoyancy; $G_{\omega b}$ is the buoyancy term; Y_ω are the dissipation of turbulence and ω; D_ω means the cross-diffusion term; G_ω means the generation of ω; σ_k and σ_ω are the turbulent Prandtl numbers for k and ω, respectively.

D. Discrete Random Walk Model

We use discrete random walk (stochastic tracking) model to predict the dispersion of asphaltene particles caused due to turbulence and the effect of instantaneous turbulent velocity fluctuations is also considered. It is assumed that the parameters, such as random velocity fluctuation (u', v', w'), time scale (τ_e), obey a Gaussian probability distribution during the lifetime of the turbulent eddy. The fluctuating velocity component u′ is expressed as:

$$u' = \varsigma \sqrt{\overline{u'^2}} \quad (15)$$

$$\sqrt{\overline{u'^2}} = \sqrt{\overline{v'^2}} = \sqrt{\overline{w'^2}} = \sqrt{2k/3} \quad (16)$$

where ζ is a normally distributed random number, and the second term on the right-hand is the local Reynolds Stress Model (RMS) value of the velocity fluctuations.

The characteristic lifetime of the eddy is defined as a constant:

$$\tau_e = 2T_L \approx 0.6 \frac{k}{\varepsilon} \quad (17)$$

III. Numerical Method

A. Geometry Generation and Mesh

In this paper, a three-dimensional computational fluid dynamic simulation is used to investigate the deposition rate of asphaltene particle through the tube with the blockage. In order to simulate the physics of real-world blockage phenomenon, the inner diameter and length of the production tubing are set as 0.062 m and 1 m, respectively. Based on the asphaltene deposition profile from caliper log in the Gulf of Mexico oilfield [27] and Rastgoo's research [28], the shape of blockage in this paper is designed. The tube with blockage is divided into three sections, including the smooth segment at the entrance and outlet and a block section in the middle of the pipe length, as shown in Fig. 1. The detail parameters of CFD simulation are shown in Table I.

TABLE I
SIMULATION PARAMETERS OF CFD

Parameters	Tube with the blockage
Diameter, m	0.062
Length, m	1
Blockage length, m	0.1, 0.2, 0.3, 0.4, 0.5
Blockage thickness, m	0, 0.005, 0.01, 0.015, 0.02
Blockage position from the tube inlet, m	0.2, 0.3, 0.4, 0.5, 0.6

Some details of unstructured mesh are shown in Fig. 2. A smooth transitional inflation layer mesh is constructed as a result of the asphaltene deposition near the wall. A fine twelve layers inflation mesh placed near the production wall is used and the growth rate is 1.2 during mesh generation. In addition, mesh independent studies are also performed, before the deposition simulation. To analyze the optimal grid independency, the max deposition rate of seven different grids ranging from 0.34 to 1.56 million are simulated in the tube without blockage. The inlet velocity is set as 3 m/s and asphaltene particle size is of 10 μm. Fig. 3 shows the plot of maximum deposition velocity variation against different number of mesh elements for the grid independency check. It can be seen that the finer mesh gives higher deposition rate, until the number of elements reached approximately 0.88 million. The maximum deposition rate of asphaltene particles at 0.88 million mesh is 3.46 kg.m^2/s whereas the deposition rate at 1.32 million mesh is 3.41 kg.m^2/s. The mean absolute error of the maximum deposition rate corresponding to the two meshes is 1.6%. This indicates that the maximum deposition velocity tends to be consistent after post 0.88 million elements. Therefore, combined with calculating cost and time, the grid independency checks through the maximum deposition rate have proved that the mesh density with 0.88 million elements gives the optimized mesh element size.

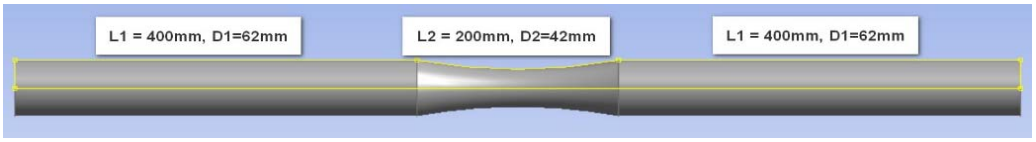

Fig. 1 Tube geometry of a tube with blockage

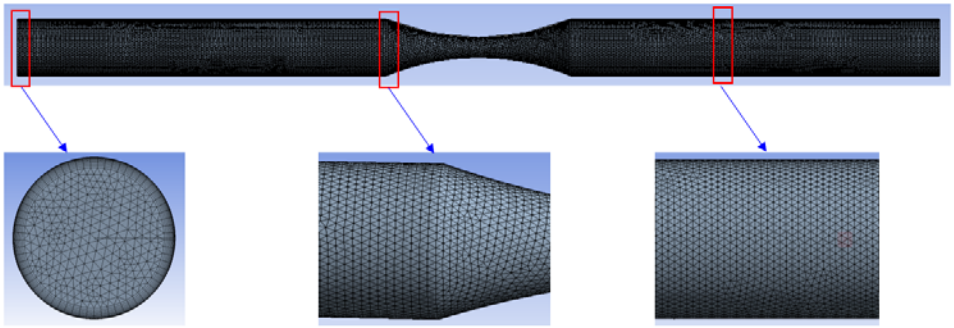

Fig. 2 Tube mesh

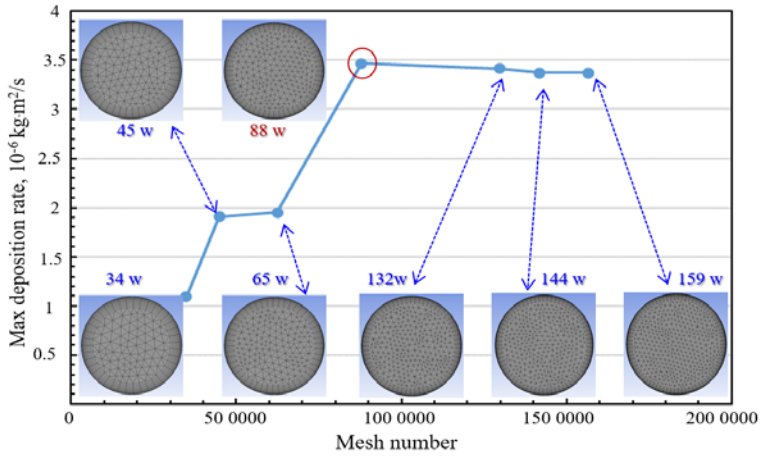

Fig. 3 Grid independence test

B. Boundary Condition

The inflow velocity is perpendicular to the inlet face and its value is equal to 3 m/s. The turbulent quantities at the tube inlet are calculated according to the turbulent intensity and the hydraulic diameter. The turbulent intensity and hydraulic

diameter are set to be 5% and 0.062 m, respectively. The inlet pressure and outlet pressure of the flow domain are equal to 20 MPa and 19.5 MPa, respectively. In addition, asphaltene particles are released uniformly from the tube inlet surface and have a same velocity with crude oil. The diameter of asphaltene particles range from 1e-5 m to 4e-4 m, distributed according to the Rosin-Rammler diameter distribution method. The density of asphaltene particle is 1100 kg/m^3 in all runs. Non-spherical drag law is adopted and the shape factor is set to 0.6. Moreover, the discrete random walk model and random eddy lifetime are used to track asphaltene particles. Since the asphaltene particles are deposited on the wall, the wall boundary condition is assumed to be trap. Such an assumption is realistic in light of the fact that the inner wall surface of wellbores retains depositing asphaltene particles. The effect of blocking segment on deposition rate is captured in the software by modifying the wall roughness. The wall motion and shear condition are set as 'stationary wall' and 'no-slip', respectively.

C. Calculation Method

In this paper, the continuity equation, conservation equations for momentum and energy of fluid flow comprise the governing equation, which is solved using the finite volume method. The Euler-Lagrangian method is used to study the deposition process of crude oil and asphaltene particles in plugged tubes. First, the Euler method is used to simulate the flow of crude oil, followed by a Lagrangian tracking of asphaltene particles passing through the system. A stochastic tracking scheme is employed to model the effects of turbulence on the deposition rate of asphaltene particles. During the process of deposition simulations, the SIMPLE algorithm is used to solve the pressure–velocity coupling scheme [29]. The second-order upwind scheme is selected for spatial discretization of the convective terms. The scaled residuals for the continuity, momentum, and energy are set to be equal to 10^{-6}. Each time, the steady-state calculation is performed for 200 steps, and then the particles are injected for transient calculation. In addition, each time step size is equal to 0.001, and the number of iterations reaches 1000. The simulation methodology is in the flow chat in Fig. 4.

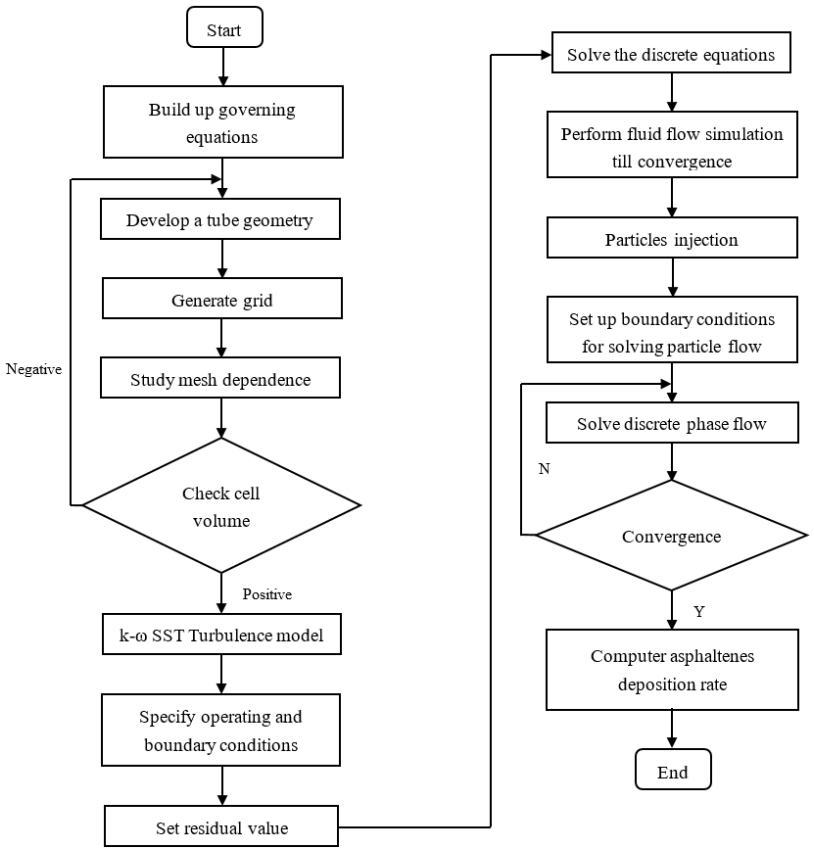

Fig. 4 Flow chart for simulation methodology

IV. CFD Simulation Results

A. Numerical Validation

Currently few experimental data sets are available for the dynamics of asphaltene deposition in wellbores blockage. Therefore, the smooth tube is selected for numerical simulation and the simulation results are compared with the experimental results to verify the accuracy of the simulation. The aerosol dynamic experiments from [30], [31], and [16] in a vertical tube were adopted to be validated. The verification results can be seen in Fig. 5. It can be seen clearly that the present deposition velocities show a good match with related literature results.

Therefore, the overall comparison indicates that the CFD simulation is accurate enough to predict deposition velocity of asphaltene particles.

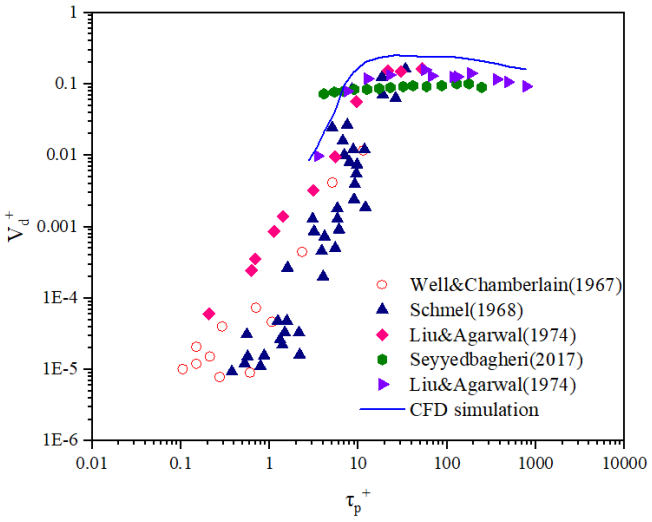

Fig. 5 Numerical validation of deposition velocity on a vertical wall

B. Sensitivity Analysis

1. Effect of Blockage Length of Blockage Tube

The blockage length is a crucial influencing factor on the deposition rate of blocked tube. In order to analyze the effect of blockage length, five different blockage lengths, 100 mm, 200 mm, 300 mm, 400 mm, and 500 mm, are selected in CFD simulation.

Figs. 6-8 depict the deposition characteristic of CFD simulation in blockage tube. According to Fig. 6, the blockage tube presents following features: Firstly, the closer to the blocked pipe, the greater the deposition rate is. This is because the particles' velocity increases with the shrinkage of the tubing, which makes it easier for the particles to deposit on the clogged pipe wall. Second, to more clearly identify the location of the maximum deposition rate, the upper limit of the maximum deposition rate in this paper is set to 2.5 E-5 kg/(m^2·s). According to the depth of the color, it can be clearly seen that the location where the deposition rate is greatest is a plugged tube of length 100 mm. Conversely, the lowest deposition rate is the blocked tube with a length of 300 mm. Finally, the asphaltene deposition distribution of clogged tube and near the outlet tube is higher than the inlet. This is because the large pressure gradient near the inlet reduces the deposition rate and amount.

All of these phenomena can also be seen in Figs. 7 and 8. Fig. 7 is the deposition rate distribution along the tube in various blockage length. The deposition distribution of asphaltenes becomes wider as the blockage length increases. Fig. 8 is the quantitative analysis of the maximum deposition rate and deposition amount in blockage tubes. It can be seen that along the length of the tube, the deposition amount and deposition rate corresponding to each plug length have the same trend. In addition, it is also found that the maximum deposition rate at the plugged length of 100 mm is greater than that at the plug length of 500 mm; however, the deposition amount at 100 mm is smaller than that at 500 mm. The reason is that the deposit thickness remains constant during the simulation, the ratio of plugged length to thickness decreases with plugged length increases, while the surface area of the plugging section increases. Consequently, it is extremely important to take into consideration the effect of blockage length on deposition rate.

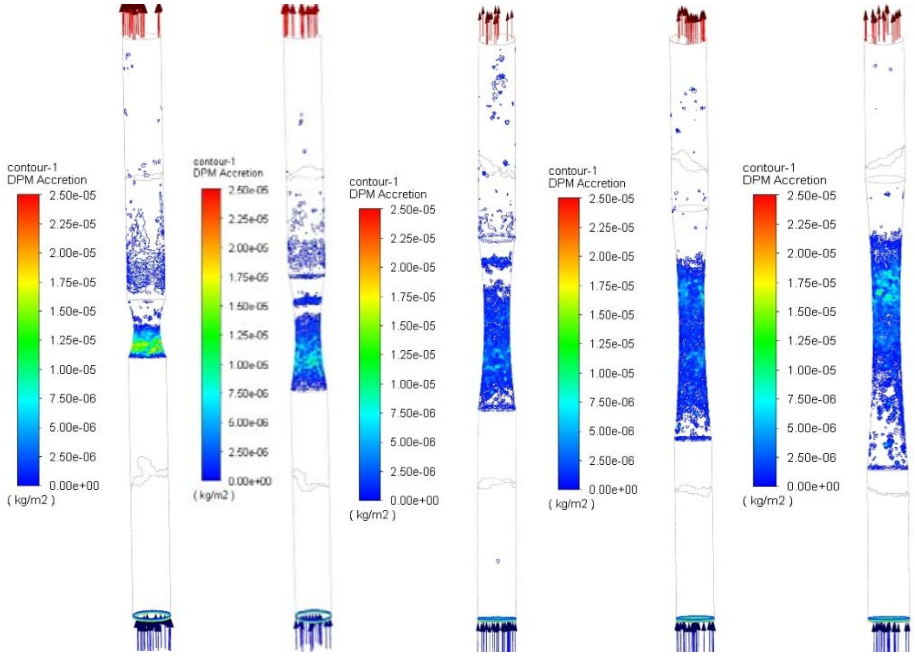

(a) 100 mm (b) 200 mm (c) 300 mm (d) 400 mm (e) 500 mm

Fig. 6 CFD simulation results with various blockage lengths

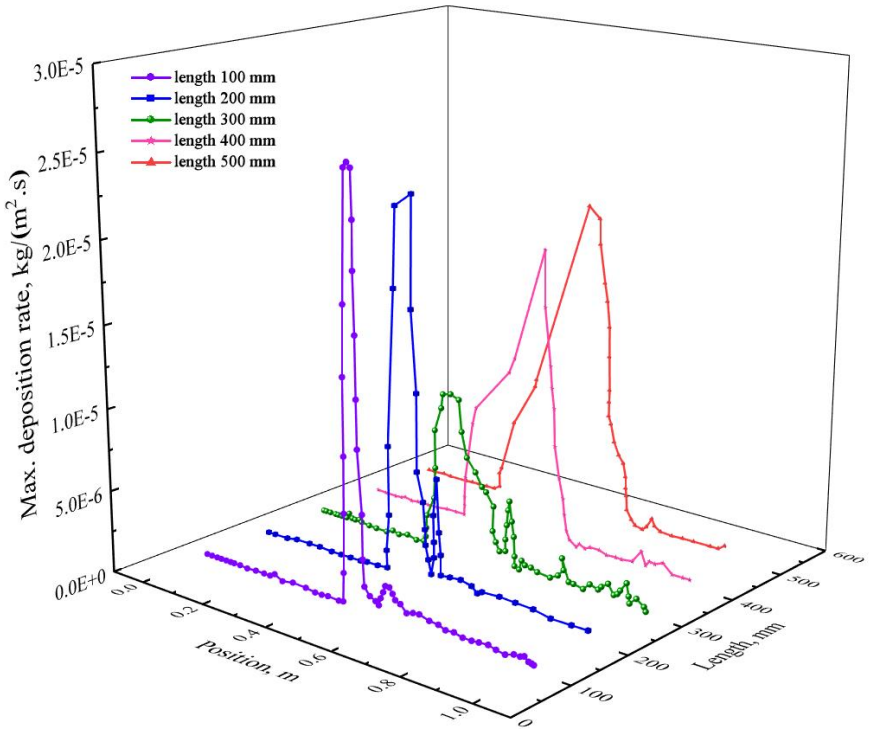

Fig. 7 Deposition rate distribution along the tube in various blockage length

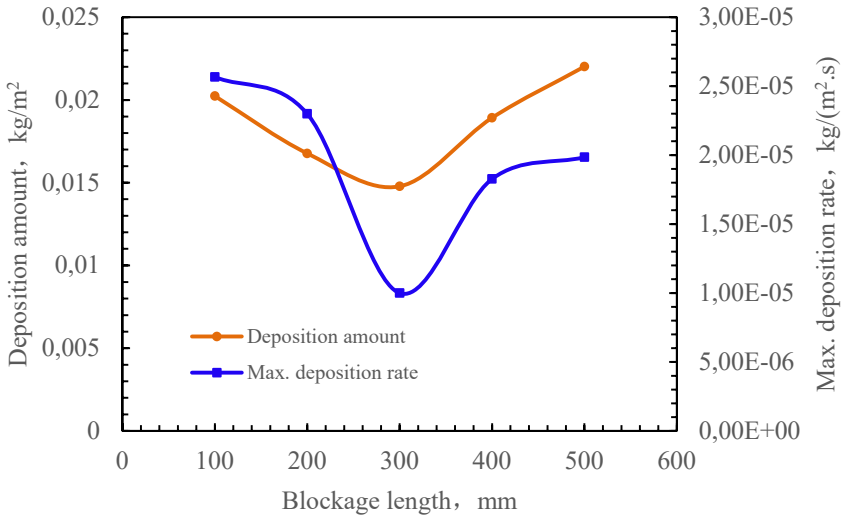

Fig. 8 Quantitative analysis of deposition amount and maximum deposition rate

2. Effect of Blockage Thickness of Blockage Tube

Under the condition that the asphaltene particle size and inlet velocity are kept constant, a parameter study with various blockage thickness, 0 mm, 5 mm, 10 mm, 15 mm, 20 mm, is also performed in CFD simulation.

Fig. 9 indicates the asphaltene deposition rate at different blockage thickness. According to Fig. 9, some conclusions can be drawn: Firstly, the greater the plugged thickness, the greater the deposition rate. Second, the deposition distribution of asphaltenes particle on the smooth pipe wall is relatively dispersed. While as the plugged thickness increases, so does the asphaltene deposition near the outlet end. The comparison of maximum deposition rate shows that the increase in blockage thickness significantly increases Max. deposition rate and deposition amount at the shrink tube and near the outlet tube end, which could require expensive intervention methods and associated production losses. Finally, we find that the Max. deposition rate of 20 mm thickness in the outlet tube is greater than that in the blocked section when the thickness is 0 and 5 mm.

In addition to the plots shown in Fig. 9, these phenomena can be also found in Figs. 10 and 11. Fig. 10 shows the Max. deposition rate distribution of asphaltene precipitation along the flow direction of the tube during the simulation. It can be clearly

seen that the Max. deposition of asphaltene particles in the plugging pipe and the outlet pipe section is abnormally significant when the blockage thickness is 20 mm. Specifically, the maximum deposition rate of the outlet pipe section of 20 mm thickness is 4.4 times and 2.8 times the maximum deposition rate when the deposition thickness is 0 mm and 5 mm, respectively. Fig. 11 displays the quantitative analysis of deposition amount and maximum deposition rate during simulation. The deposition rate and amount increase with the deposit thickness. This is because with the increase of the deposition thickness of the pipe wall, the effective flow channel of the oil flow decrease, and the asphaltene particles are more likely to deposit at the blockage tube, so that the deposition rate and deposition amount increase.

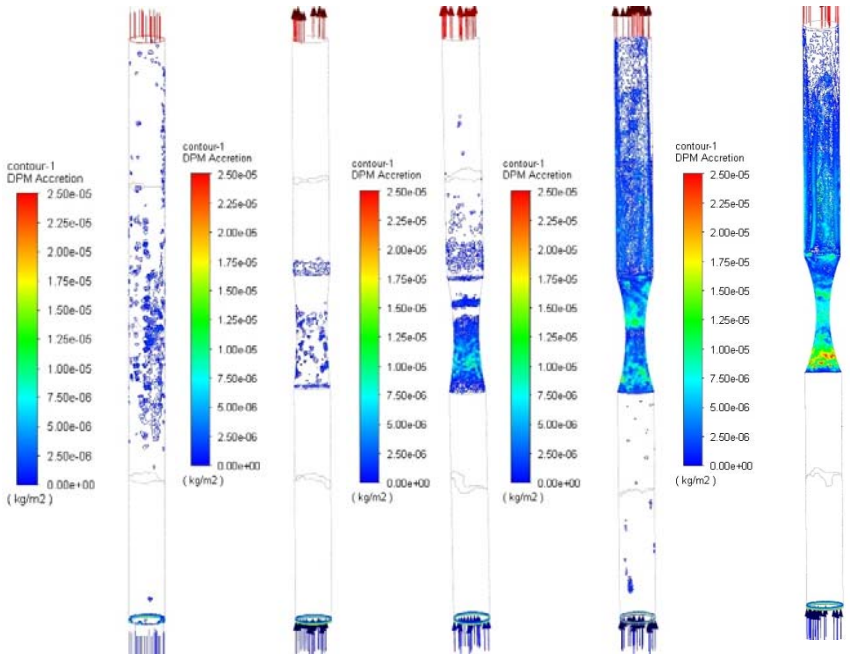

(a) 0 mm (b) 5mm (c) 10 mm (d) 15 mm (d) 20mm

Fig. 9 Effect of blockage thickness on asphaltene deposition rate

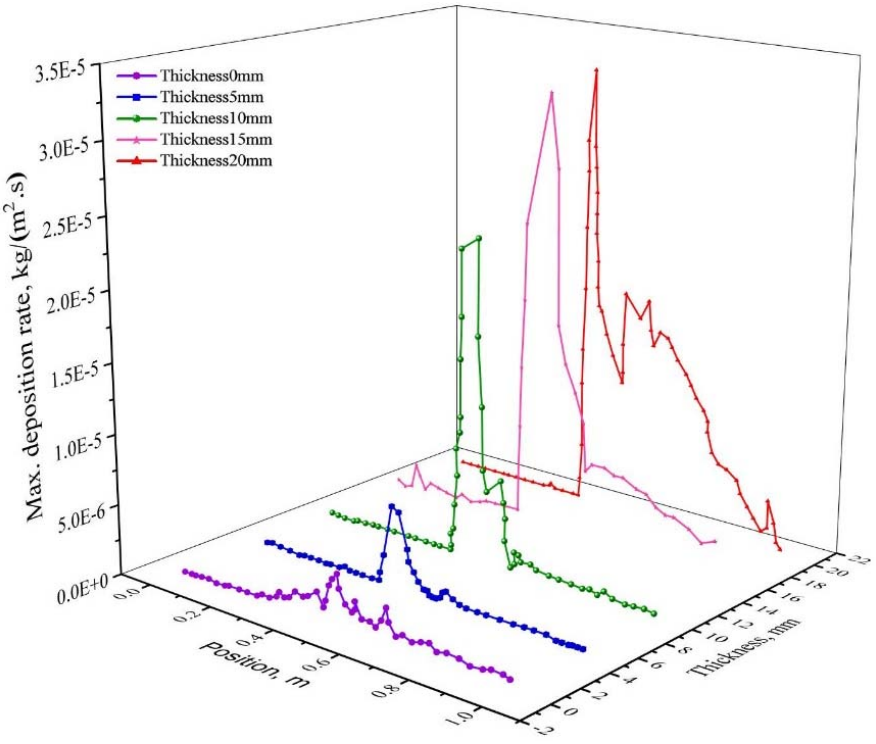

Fig. 10 Max. deposition rate distribution along the tube in various blockage thickness

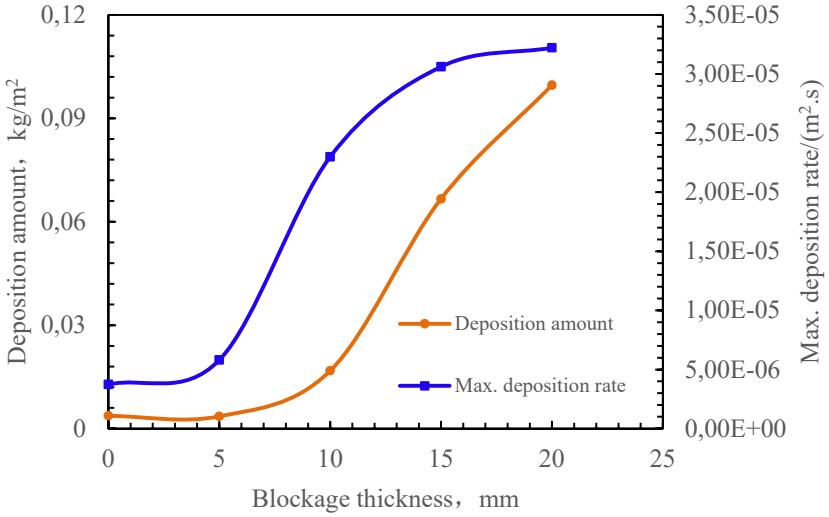

Fig. 11 Quantitative analysis of deposition amount and maximum deposition rate

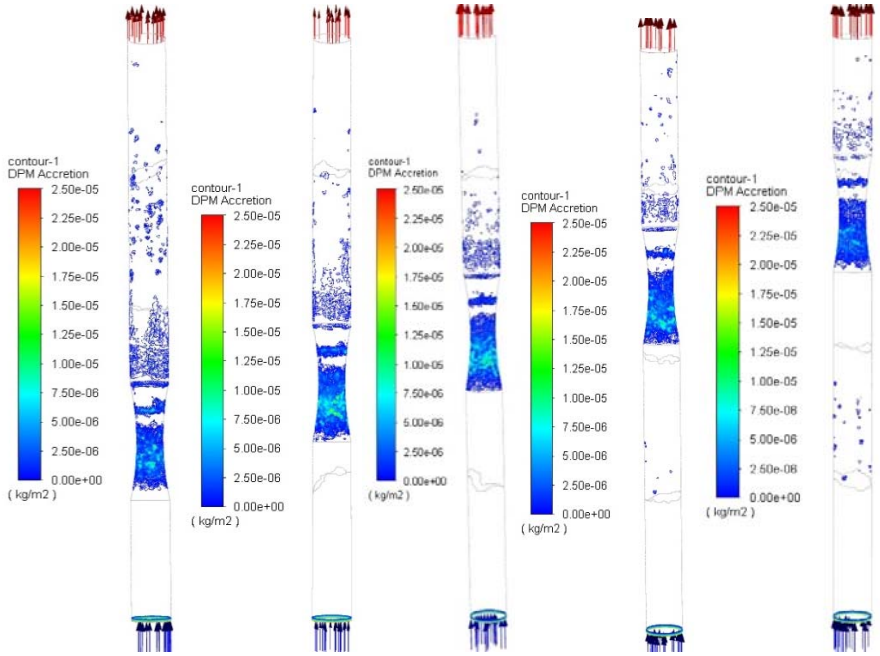

(a) Inlet 200 mm (b) Inlet 300 mm (c) Inlet 400 mm (d) Inlet 500 mm (e) Inlet 600 mm

Fig. 12 CFD simulation results with various blockage location

3. Effect of Blockage Location of Blockage Tube

The blockage location is also an important factor affecting asphaltene deposition. Because of the deposition location changes, the distribution of asphaltene deposits and the location of maximum deposition rates change. Therefore, we determine the deposition rate and deposition amount of asphaltene using CFD simulations under different blockage location, such as 200 mm, 300 mm, 400 mm, 500 mm and 600 mm from the entrance.

Fig. 12 indicates Max. deposition rate of asphaltene particles under different blockage position. As can be observed from Fig. 12, the blockage tube presents following features: Firstly, the maximum deposition rate of asphaltenes in the shrink tube is relatively close, as shown in Figs. 12 (a)-(c). Subsequently, the maximum deposition rate decreases as the deposition location is further away, as shown in Figs. 12 (d), (e). Secondly, when the asphaltene deposition position is before 400 mm, there is almost no asphaltene deposition on the smooth tube wall near the inlet, and after that, the Max. asphaltene deposition rate on the smooth tube wall near the inlet increases. Finally, as the blockage segment moves away from the inlet, the thickest asphaltene deposition position moves away. Moreover, the asphaltene deposition in the smooth tube near the inlet is relatively low.

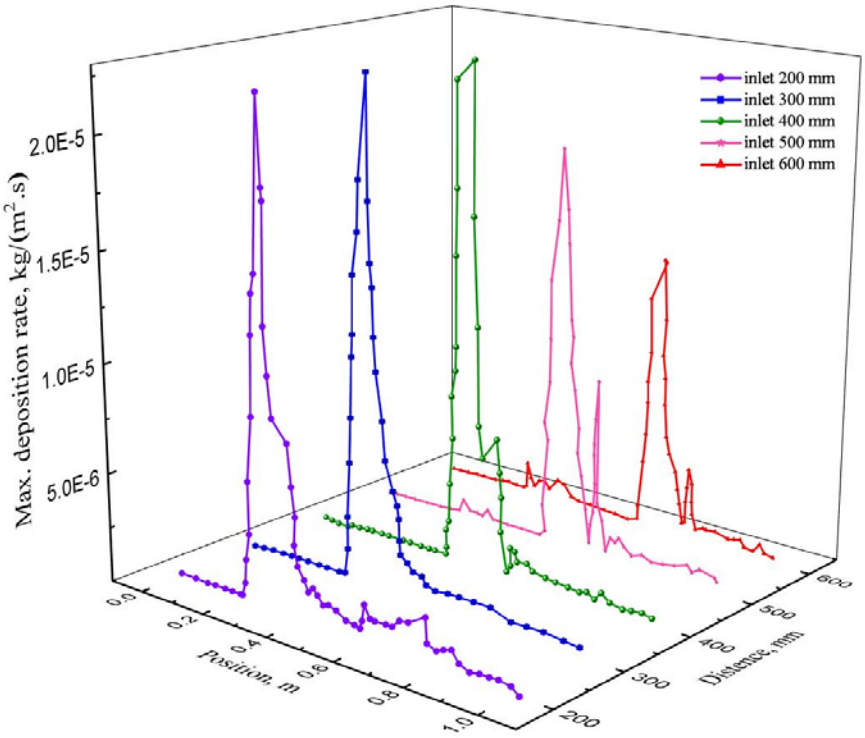

Fig. 13 Deposition rate distribution along the tube in various blockage locations

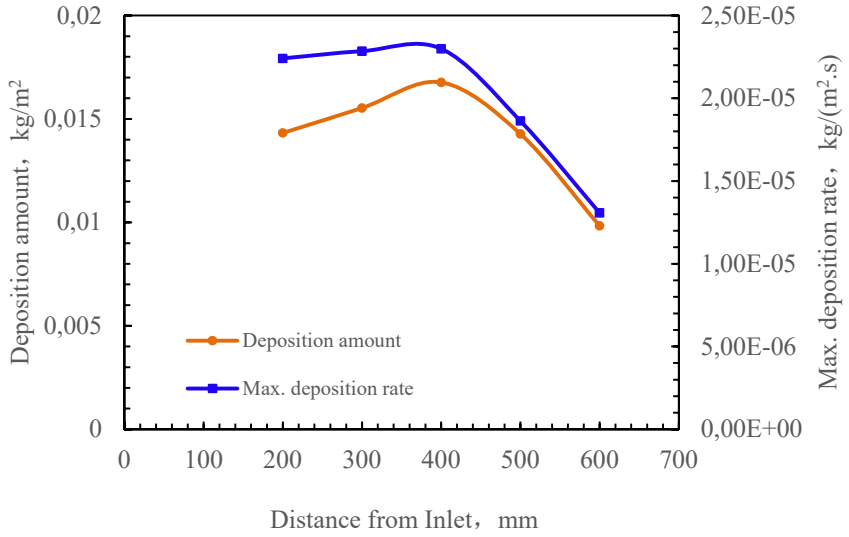

Fig. 14 Quantitative analysis of deposition amount and maximum deposition rate

In addition to the plots shown in Fig. 12, these phenomena can also be found in Figs. 13 and 14. Fig. 13 shows the distribution of asphaltene deposits along the length of the tube. It can be clearly seen that the position of the maximum deposition rate of asphaltenes moves towards the outlet. Fig. 14 is the quantitative analysis of the deposition amount and deposition rate in the asphaltene tube. The deposition amount and deposition rate have a similar trend, first increasing and then decreasing.

V. Conclusion

In this paper, the deposition rates of asphaltene particles in tube with blockage were investigated. Subsequently, the validation and sensitivity analyses of CFD simulation results are carried out. The following are the resulting conclusions of this work:

1. The closer to the blocked pipe, the greater the deposition rate is. Since the velocity of asphaltene particles increase with the tubing shrinks, resulting in particles more likely to deposit on the clogged pipe wall.

2. The asphaltene deposition distribution of clogged tube and near the outlet tube is higher than the inlet. This is because the large pressure gradient near the inlet reduces the deposition rate and amount.
3. As for blockage length concerned, the maximum deposition rate and deposition amount decrease first and then increase with the increase of plug length.
4. The maximum deposition rate of 20 mm thickness in the outlet tube is 4.4 times and 2.8 times the maximum deposition rate of 0 mm and 5 mm in the blocked section.
5. The maximum deposition rate is closer to the outlet end as the distance of blockage location increase.

Declaration of Competing Interest

We declare that we have no competing financial interests or personal relationships that could have influence the work reported in this paper.

Acknowledgement

We give special thanks to the National Natural Science Foundation of China (Grant No. 42141009) for financially supporting this research.

References

[1] A. Hosseini, E. Zare, S. Ayatollahi, et al. Electrokinetic behavior of asphaltene particles. Fuel. vol.178, no.15, pp. 234-242, 2016.
[2] Dickie, John, P., Haller, et al. Electron microscopic investigations on the nature of petroleum asphaltics. Journal of Colloid and Interface Science, vol. 29, no. 3, pp. 475-484, 1969.
[3] S. Alimohammadi, S. Zendehboudi, L. James. A comprehensive review of asphaltene deposition in petroleum reservoirs: Theory, challenges, and tips. Fuel. vol. 252, pp. 753-791, 2019.
[4] J. Escobedo, G. Ali Mansoori. Heavy-organic particle deposition from petroleum fluid flow in oil wells and pipelines. Pet. Sci. vol. 7, no. 4, pp. 502–508, 2010.
[5] C. E. Haskett, M. Tartera. A practical solution to the problem of asphaltene deposits-Hassi Messaoud field, Algeria. Journal of Petroleum Technology, vol. 17, no. 4, pp. 387–391, 1965. doi:10.2118/994-PA.
[6] D. Broseta, M. Robin, T. Savvidis, et al. Detection of asphaltene deposition by capillary flow measurements. In SPE/DOE Improved Oil Recovery Symposium. Tulsa, Oklahoma, April 2000. Doi: 10.2118/59294-MS.
[7] P. Ekholm, E. Blomberg, P. Claesson, et al. A quartz crystal microbalance study of the adsorption of asphaltenes and resins onto a hydrophilic surface. Journal of Colloid and Interface Science. vol. 247, no. 2, pp. 342-350, 2002.
[8] M. Zougari, S. Jacobs, J. Ratulowski, et al. Novel organic solids deposition and control device for live-oils: Design and applications. Energy & Fuels. Vol. 20, no. 4, pp. 1656–1663, 2006.
[9] D. Dudášová, A. Silset, J. Sjöblom. Quartz crystal microbalance monitoring of asphaltene adsorption/deposition. Journal of Dispersion Science and Technology. Vol. 29, no. 1, pp. 139–146, 2008. doi:10.1080/01932690701688904.
[10] K. Akbarzadeh, A. Hammami, A. Kharrat, et al. Asphaltenes-problematic but rich in potential. Oilfield Review. Vol. 19, no. 2, pp. 22-43, 2007.
[11] C. V. B. Favero, A. Hanpan, P. Phichphimok, et al. Mechanistic investigation of asphaltene deposition. Energy & Fuels. Vol. 30, no. 11, pp. 8915-8921, 2016. doi: 10.1021/acs.energyfuels.6b01289.
[12] J. Kuang. Simultaneous determination of asphaltene deposition and corrosion under dynamic conditions. Rice university, Houston, 2018.
[13] Zhu hj, Jing jq, Chen jw, et al. Simulations of Deposition Rate of Asphaltene and Flow Properties of Oil-Gas-Water Three-Phase Flow in Submarine Pipelines by CFD. 3rd International Conference on Computer Science and Information Technology. Vol. 5, pp. 16-22, 2010. DOI: 10.1109/ICCSIT.2010.5564116.
[14] M. Haghshenasfard, K. Hooman. CFD modeling of asphaltene deposition rate from crude oil. Journal of Petroleum Science and Engineering. vol. 128, pp. 24-32, 2015. DOI: 10.1016/j.petrol.2015.01.037.
[15] M. Jamialahmadi, B. Soltani, H. Müller-Steinhagen, D. Rashtchian, Measurement and prediction of the rate of deposition of flocculated asphaltene particles from oil, Int. J. Heat Mass Transf. 52 (2009) 4624–4634, doi: 10.1016/j.ijheatmasstransfer. 2009.01.049.
[16] H. Seyyedbagheri, B. Mirzayi. CFD modeling of high inertia asphaltene aggregates deposition in 3D turbulent oil production wells. Journal of Petroleum Science and Engineering. Vol. 150, pp. 257-264, 2017.
[17] H. Seyyedbagheri, B. Mirzayi. Eulerian Model to Predict Asphaltene Deposition Process in Turbulent Oil Transport Pipelines. Energy Fuels. Vol. 31, pp. 8061-8071, 2017. DOI: 10.1021/acs.energyfuels.7b01273.
[18] S. Emani, M. Ramasamy, K. Z. K. Shaari. Discrete phase-CFD simulations of asphaltenes particles deposition from crude oil in shell and tube heat exchangers. Applied Thermal Engineering. Vol. 149, pp. 105-118, 2019.
[19] H. Bagherzadeha, Z. Mansourpourb, B. Dabir. A coupled DEM-CFD analysis of asphaltene particles agglomeration and fragmentation. Journal of Petroleum Science and Engineering. vol. 173, pp. 402-414, 2019.
[20] R. Maddahian, A. T. Farsani, M. Ghorbani. Numerical investigation of asphaltene fouling growth in crude oil preheat trains using multi-fluid approach. Journal of Petroleum Science and Engineering. vol. 188, pp. 1-12, 2020.
[21] Gao xd, Dong pc, Chen xx, et al. CFD modeling of virtual mass force and pressure gradient force on deposition rate of asphaltene aggregates in oil wells. Petroleum Science and Technology. Vol. 40, No. 8, pp. 995-1017, 2021. DOI: 10.1080/1091 6466.021.2008972.
[22] M. Massah, E. Khamehchi, S. Mousavi-Dehghani, et al. A new theory for modeling transport and deposition of solid particles in oil and gas wells and pipelines. International Journal of Heat and Mass Transfer. 152 (2020): 1-11.
[23] S. Kord, O. Mohammadzadeh, R. Miri, et al. Further investigation into the mechanisms of asphaltene deposition and permeability impairment in porous media using a modified analytical model. Fuel, vol. 117, no. 30, pp. 259-268, 2014.
[24] S. Elghobashi. Particle-laden turbulent flows: direct simulation and closure models. Applied Scientific Research. Vol. 48, pp. 301-314, 1991.
[25] A. Haider, O. Levenspiel. Drag Coefficient and Terminal Velocity of Spherical and Nonspherical Particles". Powder Technology. Vol. 58, no. 1, pp. 63–70, 1989.
[26] P. G. Saffman. The lift on a small sphere in a slow shear flow. Journal of Fluid Mechanics. Vol. 22, pp. 385–400, 1965.
[27] C. E. Haskett, M. Tartera. A Practical Solution to the Problem of Asphaltene Deposits-Hassi Messaoud Field, Algeria. J Pet Technol. Vol. 17, no. 4, pp. 387–391, 1965.
[28] A. Rastgoo, R. Kharrat. Investigation of Asphaltene Deposition and Precipitation in Production Tubing. International Journal of Clean Coal and Energy. Vol. 6, no.1, pp. 14-29, 2017. Doi: 10.4236/ijcce. 2017.61002.
[29] S. V. Patankar. Numerical heat transfer and fluid flow. Hemisphere Publishing, Washington, D.C.1980.
[30] B. Y. Liu, J. K. Agarwal. Experimental observation of aerosol deposition in turbulent flow. J. Aerosol Sci. vol. 5, pp. 145–155, 1974.
[31] A. C. Wells1, A. C. Chamberlain. Transport of small particles to vertical surfaces. Journal of Applied Physics. Vol. 18, no. 12, pp. 1793-1799, 1967.